M. (1989) *Biochemistry 28*, 5058.
Spiro, T. G., & Li, X.-Y. (1988) in *Biological Applications of Raman Spectroscopy*, Vol. 3, Chapter 1, Wiley-Interscience, New York.
Suzuki, M., Yokoyama, T., & Ito, M. (1968) *Spectrochim. Acta 24A*, 1091.
Thaller, C., Weaver, L. H., Eichele, G., Wilson, E., Karlsson, R., & Jansonius, J. N. (1981) *J. Mol. Biol. 147*, 465-469.
Wilson, E. B., Jr., Decius, J. C., & Cross, P. C. (1980) *Molecular Vibrations*, Dover Publications, New York.
Yonetani, T. (1976) *Enzymes (3rd Ed.) 13*, 345-361.
Yonetani, T., & Anni, H. (1987) *J. Biol. Chem. 262*, 9547.

Structure of a Thermostable Disulfide-Bridge Mutant of Phage T4 Lysozyme Shows That an Engineered Cross-Link in a Flexible Region Does Not Increase the Rigidity of the Folded Protein[†,‡]

P. E. Pjura, M. Matsumura, J. A. Wozniak, and B. W. Matthews*
Institute of Molecular Biology and Department of Physics, University of Oregon, Eugene, Oregon 97403
Received August 16, 1989; Revised Manuscript Received October 12, 1989

ABSTRACT: A disulfide bond introduced between amino acid positions 9 and 164 in phage T4 lysozyme has been shown to significantly increase the stability of the enzyme toward thermal denaturation [Matsumura, M., Becktel, W. J., Levitt, M., & Matthews, B. W. (1989) *Proc. Natl. Acad. Sci. U.S.A. 86*, 6562-6566]. To elucidate the structural features of the engineered disulfide, the crystal structure of the disulfide mutant has been determined at 1.8-Å resolution. Residue 9 lies in the N-terminal α-helix, while residue 164 is located at the extreme C terminus of T4 lysozyme, which is the most mobile part of the molecule. The refined structure shows that the formation of the disulfide bond is accompanied by relatively large ($\sim$2.5 Å) localized shifts in C-terminal main-chain atoms. Comparison of the geometry of the engineered disulfide with those of naturally observed disulfides in proteins shows that the engineered bridge adopts a left-handed spiral conformation with a typical set of dihedral angles and C_α–C_α distance. The geometry of the engineered disulfide suggests that it is slightly more strained than the disulfide of oxidized dithiothreitol but that the strain is within the range observed in naturally occurring disulfides. The wild-type and cross-linked lysozymes have very similar overall crystallographic temperature factors, indicating that the introduction of the disulfide bond does not impose rigidity on the folded protein structure. In particular, residues 162-164 retain high mobility in the mutant structure, consistent with the idea that stabilization of the protein is due to the effect of the disulfide cross-link on the unfolded rather than the folded state. The 9-164 disulfide bridge, as well as other disulfides in T4 lysozyme, were introduced into a pseudo-wild-type molecule in which the naturally occurring cysteines at positions 54 and 97 were replaced, respectively, with threonine and alanine. The structure of this pseudo-wild-type lysozyme has also been determined at high resolution and shown to be very similar to that of the normal wild-type molecule.

It has been shown for many naturally occurring proteins that disulfide bonds can considerably enhance stability (Anfinsen & Scheraga, 1975; Johnson et al., 1978; Goto & Hamaguchi, 1979; Lin et al., 1984; Ueda et al., 1985; Creighton, 1986; Schwarz et al., 1987; Pace et al., 1988; Lin & Kim, 1989). This large stabilizing potential has made the engineering of nonnative disulfide bonds into proteins an attractive strategy for the improvement of protein stability. Such attempts include dihydrofolate reductase (Villafranca et al., 1983, 1987), T4 lysozyme (Perry & Wetzel, 1984, 1986; Wetzel et al., 1988; Matsumura & Matthews, 1989; Matsumura et al., 1989a,b), subtilisin (Wells & Powers, 1986; Mitchinson & Wells, 1989; Pantoliano et al., 1987), and λ-repressor (Sauer et al., 1986). In all cases the newly introduced cysteines were found to form disulfide bonds, albeit more or less readily in different instances. However, the addition of new disulfides did not always confer an increase in stability relative to that of wild type. One of the reasons for this modest success appears to be the difficulty in finding sites within a protein where the geometry is optimal for introduction of a disulfide bridge. Also, the advantage of the cross-link cannot be fully realized if it leads to proteolysis (Wells & Power, 1986; Mitchinson & Wells, 1989) or intermolecular thiol/disulfide interchange evoked by a third cysteine residue (Perry & Wetzel, 1986; Villafranca et al., 1987).

Recently, four different nonnative disulfide bonds (residues 9-164, 21-142, 90-122, and 127-154) were introduced into a cysteine-free T4 phage lysozyme (Matsumura et al., 1989). The 9-164 and 21-142 disulfide mutants were more thermostable than wild type, whereas the other two mutants were slightly less stable. Measurement of stability of the engineered disulfide bonds to reduction by dithiothreitol (DTT) indicated that the presumed stabilization of the native structure by the reduction in entropy of the unfolded protein (Schellman, 1955; Flory, 1956; Poland & Scheraga, 1965; Chan & Dill, 1989) appeared to be offset by two factors: (1) the disruption or loss of preexisting interactions in wild-type structure due to introduction of new cysteine(s) and (2) the energetic constraints associated with disulfide formation in the native structure. Although the net stability of the engineered protein is determined by the combination of these three factors, from the point

[†] This work was supported in part by a grant from NIH (GM21967 to B.W.M.) and by the Lucille P. Markey Charitable Trust.
[‡] The atomic coordinates in this paper have been submitted to the Brookhaven Protein Data Bank.

0006-2960/90/0429-2592$02.50/0

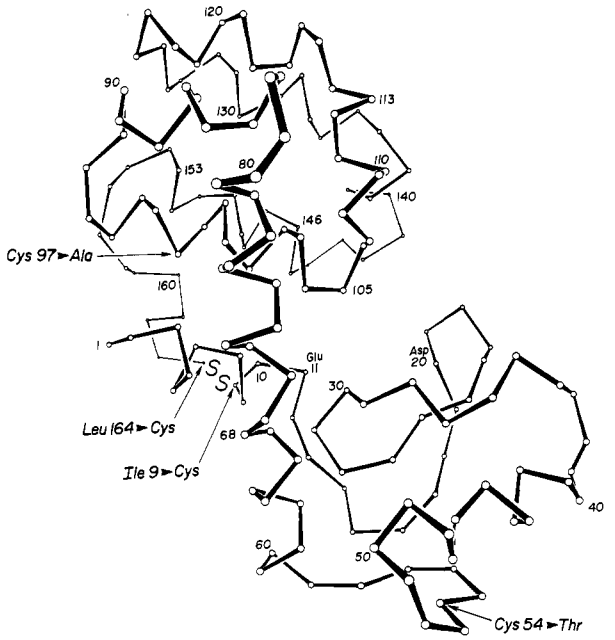

FIGURE 1: Schematic view of the α-carbon backbone of bacteriophage T4 lysozyme, showing the locations of the mutations Ile 9 → Cys and Leu 164 → Cys that form the disulfide bridge. The two cysteines were introduced into a cysteine-free pseudo-wild-type lysozyme (54T-97A or WT*). The locations of the auxiliary mutations Cys 54 → Thr and Cys 97 → Ala are also shown.

of view of protein engineering the constraint imposed by the disulfide geometry is perhaps the most limiting factor. Destabilization due to the introduction of new cysteines can be minimized by avoiding the replacement of bulky, buried residues. As judged by the observed stabilities of the reduced forms of mutant T4 lysozymes, this term was less than 2 kcal/mol in the worst case. In contrast, the entropic stabilization theoretically expected from each cross-link is 3.8–5.4 kcal/mol (Pace et al., 1988). Thus, if no strain were associated with disulfide bond formation, all the disulfide mutants should have been stabilized relative to wild type. However, the measurement of redox potentials of the engineered disulfide bonds indicated that each of the disulfide bridges was unfavorable, relative to DTT, by 1.2–4.2 kcal/mol. In the cases of the 90–122 and 127–154 disulfide mutant lysozymes, which are less stable than wild type, the larger strain energies (2.4–4.2 kcal/mol relative to DTT) appeared to be the major factor offsetting the favorable entropic stabilization. The two most effective disulfide bonds in T4 lysozyme were under less strain (1.2–2.1 kcal/mol relative to DTT) (Matsumura et al., 1989a).

To understand how the structural constraints of the disulfide bonds in these engineered lysozymes relate to their stabilities, the X-ray structure of the 9–164 disulfide mutant has been determined at 1.8-Å resolution. The location of the disulfide bridge relative to the overall molecular structure of T4 lysozyme is shown in Figure 1. Topologically, the loop formed by the disulfide bridge encloses almost the whole molecule. In terms of the folded structure, however, the N-terminal α-helix (residues 3–10) interacts much more extensively with the "upper" (C-terminal) domain than with the "lower" (N-terminal) domain (Figure 1). Therefore, from a structural point of view, the 9–164 bridge can be considered as within the C-terminal domain.

Experimental Methods

Mutagenesis and Protein Purification. The disulfide mutant of T4 lysozyme (Ile 9 to Cys, Cys 54 to Thr, Cys 97 to Ala, and Leu 164 to Cys; designated 9C-164C-WT*) was obtained by site-directed mutagenesis using the uracil-template procedure of Kunkel et al. (1987) as previously described (Matsumura et al., 1989a). The mutant gene was cloned into the plasmid pHSe5 (Muchmore et al., 1989) and used to transform *Escherichia coli* RR1. The mutant lysozyme was overproduced by the addition of isopropyl β-thiogalactoside.

The protein was isolated as previously described (Alber & Matthews, 1987). In brief, the EDTA-lysed cells and the supernatant of centrifuged growth medium, which contains lysozyme released from prematurely lysed cells, were dialyzed against distilled water and applied to a CM-Sephadex column, and the protein was eluted by using a 50–300 mM NaCl gradient in 50 mM phosphate buffer. The peak fractions were collected, dialyzed, and adsorbed on a SP-Sephadex column. The concentrated protein was eluted with 0.1 M NaCl in the buffer. Typical yields were 40–50 mg from 1 L of growth medium.

Crystallization. Crystals were grown by using the microbatch method. To 25 μL of protein (15.5 mg/mL) in 0.1 M NaH_2PO_4, 0.55 M NaCl, and 0.02% NaN_3 (pH 6.5) in silanized glass vials was added 26 μL of 4 M Na/KPO_4 and 10 mM 2-mercaptoethanol, pH 6.5. Small crystals, 0.1–0.2 mm on edge, appeared after 1 week; these grew to 0.6 mm on edge after 5 months. The crystals are in the trigonal space group $P3_221$ and are isomorphous with the wild-type crystals (Weaver & Matthews, 1987). The fully grown crystals were equilibrated with standard mother liquor containing 1.05 M K_2HPO_4, 1.26 M NaH_2PO_4, 0.23 M NaCl, and 1.4 mM 2-mercaptoethanol, pH 6.7.

Data Collection and Refinement. Twenty film packs were collected from two crystals of the 9C-164C-WT* mutant lysozyme on a Rigaku Rotaflex RU-200BH rotating anode X-ray generator (Cu Kα radiation at 40 kV × 150 mA), using the rotation method as described by Schmid et al. (1981). Ten 2° exposures were collected from each crystal at 3.5 h/exposure. The crystals diffracted to a resolution of 1.8 Å. The films were scanned on an Optronics System P-1000 photoscanner, and the data were evaluated by using the method of Rossmann (1979) as adapted by Schmid et al. (1981).

Similar procedures were used to measure data to 1.8-Å resolution for the pseudo-wild-type (Cys 54 → Thr and Cys 97 → Ala, designated WT*) lysozyme. Data processing statistics are summarized in Table I.

The structures were refined by using the TNT package of restrained least-squares refinement routines (Tronrud et al., 1987), together with model building on an Evans and Sutherland PS330 graphics station using the molecular modeling program FRODO (Jones, 1982). First, the coordinates of the

Table I: Data Processing and Refinement Statistics[a]

protein	54T-97A(WT*)	9C-164C-WT*
cell dimensions		
a, b (Å)	60.9	61.2
c (Å)	97.1	96.9
unique reflections	14975	14686
resolution (Å)	1.8	1.8
R_{merge} (%)	7.0	6.9
R (%)	16.6	15.7
Δ_{bond} (Å)	0.019	0.014
Δ_{angle} (deg)	2.7	1.98

[a] 54T-97A(WT*) is the cysteine-free pseudo-wild-type lysozyme created by replacing Cys 54 with threonine and Cys 97 with alanine. 9C-164C-WT* is the disulfide-bridged lysozyme obtained by introducing the substitutions Ile 9 → Cys and Ile 164 → Cys into WT*. R_{merge} is the agreement between intensities measured on different films. R is the crystallographic residual for the refined structure. Δ_{bond} and Δ_{angle} are the root mean square deviations of bond length and angles from ideal stereochemistry (Tronrud et al., 1987).

cysteine-free pseudo-wild-type protein were refined in a straightforward manner starting with the refined coordinates of normal wild-type lysozyme (Weaver & Matthews, 1987). These coordinates were then used as a starting model for the disulfide mutant in which residues Ile 9 and Leu 164 were initially replaced with alanine residues. The starting R factor was 22.3%. The model was subjected to an initial round of positional refinement, with special attention being given to the three C-terminal residues (162–164). The R factor was reduced to 16.7%. At this stage, the disulfide bond near residues 9 and 164 was clearly defined in the $F_o - F_c$ density map. Then, two cysteines were added to the model such that the two sulfur atoms were at the center of their respective lobes of density. Several more rounds of positional and temperature-factor refinement were performed, using FRODO to make adjustments to the model as necessary, until the R factor converged and no further corrections could be made. To test whether the disulfide geometry was influenced by the stereochemical constraints of the refinement program, no sulfur–sulfur bond restraint was applied during the first and last rounds of refinement; there was essentially no difference in geometry whether this restraint was applied or removed. The relevant refinement statistics are listed in Table I. Coordinates for the refined structures have been deposited in the Brookhaven Protein Data Bank.

Results

The refined structure of cysteine-free pseudo-wild-type (WT*) lysozyme is very similar to that of wild-type lysozyme, except in the vicinity of the mutations Cys 54 → Thr and Cys 97 → Ala. At amino acid position 97, both the backbone and side-chain structures of WT* lysozyme appear to be identical with that of wild type except for the deletion of the γ-sulfur atom. At position 54 the γ-methyl group of the replacement threonine is located at virtually the same position as occupied by the γ-sulfur atom of Cys 54 of wild-type lysozyme. The extra γ-hydroxyl group of the threonine is accommodated in the interior of the WT* protein without disturbing the backbone structure. This introduced hydroxyl group appears to form hydrogen bonds to the carboxyl group (OD1) of Asp 47 (2.6 Å) and the amides of Asn 55 (3.1 Å) and Gly 56 (3.3 Å). In addition to its structural similarity to normal wild-type lysozyme, the pseudo-wild-type lysozyme also has activity and stability that are essentially identical with those of the wild-type enzyme (Matsumura & Matthews, 1989; Matsumura et al., 1989a).

The difference electron-density map between the mutant (9C-164C-WT*) and pseudo-wild-type (WT*) lysozyme (Figure 2a) shows several significant features in the vicinity of the expected disulfide bridge. The largest is a bilobate positive feature with peak-to-peak separation of 2.1 Å, agreeing with the expected sulfur–sulfur distance (2.05 Å). Two large negative peaks are seen at the sites corresponding to the side-chain atoms of residues Ile 9 and Leu 164 in the WT* structure, indicating the replacement of residues 9 and 164 with cysteines. There are also smaller positive peaks near the carbonyl oxygen of residue 9, the carbonyl group of residue 10, and along the backbone atoms of residues 162–164, suggesting that there has been a shift of these residues toward the disulfide bond in the mutant structure. These features all indicate that the 9C-164C-WT* mutant forms a disulfide bond between residues 9 and 164. There are no other significant difference features seen elsewhere in the map.

The positions of residues 162–164 were of special concern during the refinement. In wild-type as well as other mutant lysozyme structures, these residues are poorly defined, apparently due to disorder or extreme thermal motion (Weaver & Matthews, 1987). Because residue 164 was constrained by the disulfide bond, we expected that residues 162–164 might be more clearly delineated. However, the $2F_o - F_c$ electron density for these residues in the mutant structure was also very weak, with a break between the N and CA atoms of residue 163. Initial attempts to fit the backbone to this density resulted in sterically unacceptable backbone conformations. To confirm the position of the C-terminal backbone, an "omit map" was calculated by using the coordinate set with residues 162–164 deleted. The resulting map (Figure 2b) shows essentially continuous positive difference density, defining the positions of the residues. The omit map also indicates that there is a substantial shift in the position of residue 163. Adjusting the model to fit this density resolved the problem of steric interference between the residues. Nevertheless, the adjustment of the backbone structure did not eliminate the N–CA break at residue 163 in the $2F_o - F_c$ map, even after the refinement was complete. Although the reason for this discontinuity is uncertain, we feel that the evidence from the omit map (Figure 2b), together with the features seen in the $F_{mutant} - F_{WT*}$ map (Figure 2a), supports the modeling of the C terminus, both in the mutant and in the WT* structures.

Figure 2c shows the refined structure of the 9C-164C-WT* mutant. Following the surveys of Richardson (1981) and Thornton (1981), the 9–164 disulfide takes the form of a left-handed spiral. On the residue 164 side of the disulfide the dihedral angles are $\chi_1' = -76°$ and $\chi_2' = -78°$, which correspond to a near-perfect spiral. On the residue 9 side, however, the dihedral angles are $\chi_1 = -163$ and $\chi_2 = 157$, which indicates a substantial departure from the idealized spiral conformation. The sulfur–sulfur torsion angle is $\chi_3 = -106°$, which is reasonably close to the expected value of about $-90°$. Other than the χ_1 and χ_2 dihedral angles the disulfide is essentially undistorted, with bond lengths and angles all close to idealized values and with no bad van der Waals contacts between the cross-link and adjacent residues in the protein structure.

The two regions of backbone connected by the disulfide linkage have the form of a helix and a distorted, helix-like region crossing each other at an oblique angle. The helix that includes residue 9 consists of a well-defined, α-like helix spanning residues 3–10. The backbone near residue 164, on the other hand, has a quite irregular conformation, consisting of a hairpin bend starting at residue 159 and extending to residue 162, where it flares out to form the cross-link. The stretch is somewhat helical at the end of the chain, though it does not appear to make any of the interhelical hydrogen bonds between carbonyl oxygens and amide nitrogens seen in a normal helix. This overall pattern is like that seen by Richardson (1981) for two helices connected by a disulfide in which the helices cross at 60–90° angle, with one of the helices usually being distorted while the other is essentially normal.

To compare the 9C-164C-WT* mutant and WT* structures, least-squares superposition of the mutant main-chain atoms onto the WT* structure was carried out by using the transformation

$$X' = 0.99997X + 0.00413Y - 0.00625Z - 0.069$$
$$Y' = -0.00409X + 0.99997Y + 0.00586Z + 0.046$$
$$Z' = 0.00628X - 0.00583Y + 0.99996Z - 0.198$$

The root mean square difference between the main-chain atoms in the two structures after superposition is 0.13 Å. As shown in Figure 2d, residues 162–164 appear to have undergone a substantial conformational rearrangement (up to 2.5 Å) to accommodate the geometric requirements of the

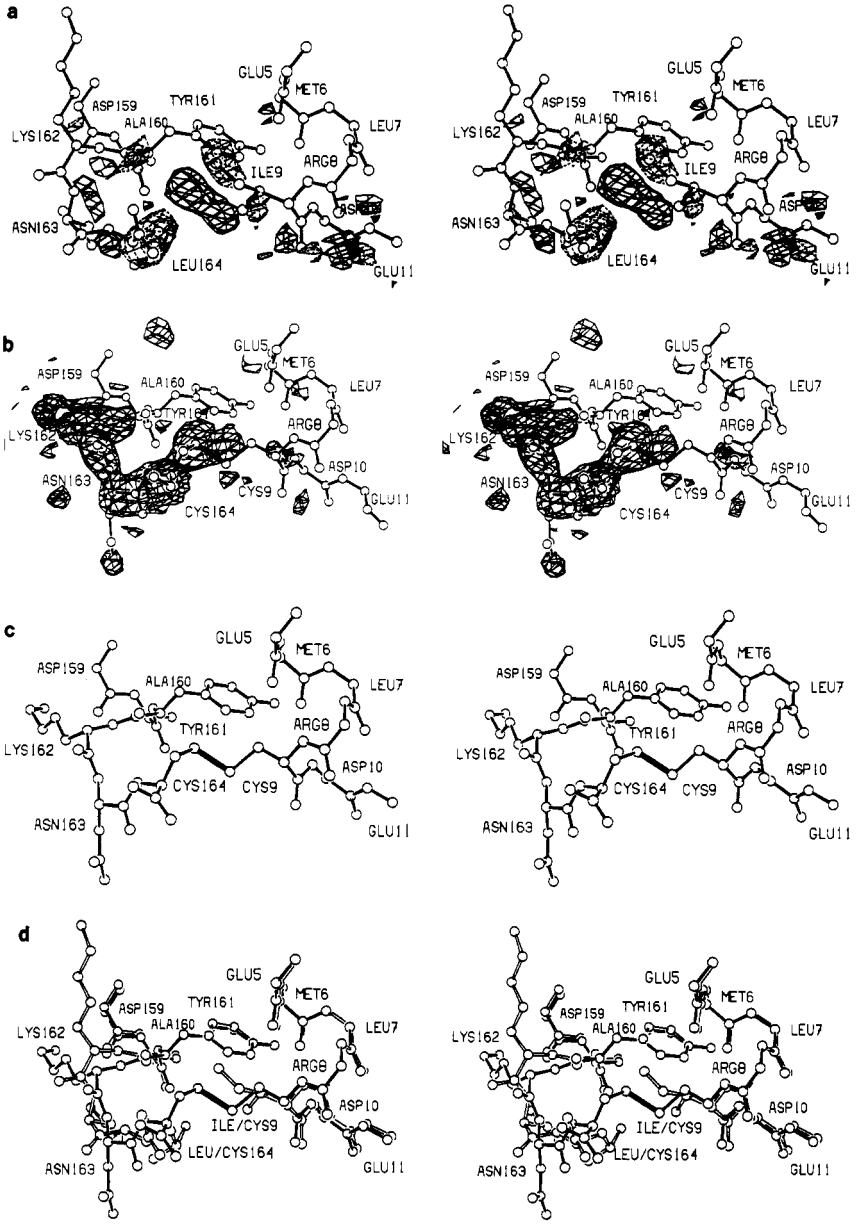

FIGURE 2: (a) Stereo drawing of the difference in electron density between the 9–164 disulfide mutant (9C-164C-WT*) and pseudo-wild-type (WT*) lysozyme in the vicinity of the mutations Ile 9 → Cys and Leu 164 → Cys, superimposed on the structure of WT* lysozyme. The difference electron density is calculated with amplitudes $F_{9C\text{-}164C\text{-}WT^*} - F_{WT^*}$, where $F_{9C\text{-}164C\text{-}WT^*}$ and F_{WT^*} are the observed structure amplitudes for the 9–164 disulfide mutant and pseudo-wild-type lysozyme, respectively. Phases are from the refined pseudo-wild-type structure. Resolution is 1.8 Å. The negative density (broken lines) and positive density (solid lines) are contoured at $\pm 4\sigma$, where σ is the root mean square difference density throughout the unit cell. (b) Stereo drawing showing an "omit" electron density map of the 9–164 disulfide mutant lysozyme in the vicinity of the disulfide bridge. The difference electron density is calculated with amplitudes $(F_o - F_c)$, where F_o is the observed structure amplitude for the 9–164 disulfide mutant and F_c and the phases are calculated for the mutant structure by deleting the C-terminal residues 162–164. The positive density is contoured at height of $+2\sigma$. (c) Stereo drawing showing the refined structure of the 9–164 disulfide mutant lysozyme. The disulfide bond between the sulfur atoms of Cys 9 and Cys 164 is indicated by a bold line. (d) Superposition of the refined structure of the 9–164 disulfide mutant (solid bonds) on pseudo-wild-type lysozyme (open bonds).

disulfide linkage, while residue 9 has simply shifted slightly (~0.4 Å) toward the bond without undergoing any significant conformational change. Figure 3 shows the apparent shift of every α-carbon atom of the mutant structure relative to WT* lysozyme. There is no evidence for significant structural change elsewhere in the structure.

An analysis of the average main-chain temperature factors for residues in the mutant and WT* structures provides an explanation for the asymmetry of the apparent structural changes. In the WT* structure, the thermal factors for residues 9 and 161 are both around 20 Å^2, which is a typical value for most sections of the main chain and shows that these residues are not unusually mobile. On the other hand, the temperature factors for residues 162–164 are in the range 60–70 Å^2, which indicates that these residues are, by contrast, highly mobile. In the 9C-164C-WT* mutant the corresponding temperature factors for the backbone are virtually identical—residues 9 and 161 still have low temperature values, while residues 162–164 maintain high values, despite the fact that residue 164 is now connected to residue 9 by the disulfide linkage. Thus, the high conformational flexibility of the carboxy terminus seen in the WT* structure is retained in the mutant.

As was noted in the refinement of wild-type lysozyme, the high thermal factors of residues 162–164 prevent the coordinates of these residues from being determined reliably (Weaver & Matthews, 1987). On the other hand, the presence of obvious negative density in Figure 2a at the presumed site

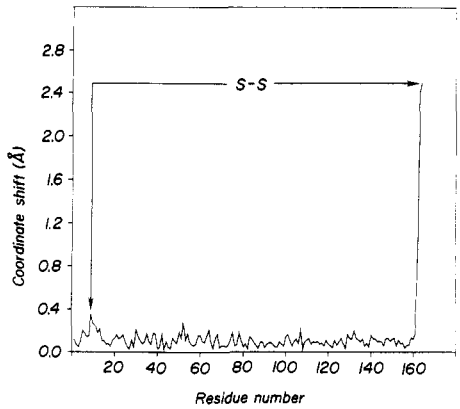

FIGURE 3: Shift plot showing the difference in the refined coordinates of the α-carbon atoms of pseudo-wild-type and 9–164 disulfide mutant lysozymes. Prior to this comparison, the coordinates of the 9–164 disulfide mutant were rotated and translated to eliminate changes in the unit cell dimensions and any other global differences (see text). The residues connected by the disulfide bridge are indicated.

of Ile 164 side chain tends to confirm that this residue was located in roughly the correct location. Nevertheless, the apparent high mobility of residues 162–164 in both the wild-type and mutant structure means that the coordinates of these residues must be regarded with caution.

Discussion

(A) Effect of the Disulfide Bond on the Native Structure. The stabilizing effect of any type of covalent cross-link in a protein structure has been attributed predominantly to the reduction in chain entropy of the unfolded state (Schellman, 1955; Flory, 1956; Poland & Scheraga, 1965; Chan & Dill, 1989). This idea has been tested for various proteins, and the results have shown that cross-links can provide approximately the expected degree of the stabilization (Anfinsen & Scheraga, 1975; Johnson et al., 1978; Goto & Hamaguchi, 1979; Lin et al., 1984; Pace et al., 1988). However, in many instances the entropic effect alone does not account for the observed change in stability due to the cross-link (Ueda et al., 1985; Goldenberg, 1985; Creighton, 1986; Goto & Hamaguchi, 1986; Goto et al., 1987). These experiments indicate that the cross-link can have an important effect not only on the unfolded state but on the folded state as well. In particular, a disulfide bridge can destabilize the folded protein because of geometric constraints due to the covalent cross-linkage (Ueda et al., 1985) and steric distortion due to the change in side-chain volume that occurs when an oxidized disulfide bond is reduced (Thornton, 1981; Goto & Hamaguchi, 1986).

(1) Disulfide Geometry. The strain energy associated with genetically engineered disulfide bridges can be analyzed, at least in part, by comparing the structural features of engineered disulfide bonds with those of naturally occurring disulfide bonds. One of the most characteristic parameters for a disulfide bond is the dihedral angle around the S–S bond (χ_3). In naturally occurring proteins, there are equal numbers of left-handed ($\chi_3 \simeq -90°$) and right-handed disulfides ($\chi_3 \simeq +90°$) (Richardson, 1981; Thornton, 1981). The average C_α–C_α distance for left-handed disulfides is 6.1 Å, while for the right-handed ones the average C_α–C_α distance is 5.2 Å. The χ_3 value of the 9–164 disulfide bond is −106°, and the C_α–C_α distance is 5.8 Å, showing that the engineered disulfide belongs to the left-handed spiral conformation and has a normal C_α–C_α' separation.

In Figure 4 the side-chain dihedral angles (χ_1, χ_2, χ_3, χ_2', and χ_1') and the C_α–C_α distance for the 9–164 disulfide are compared with those of left-handed disulfides in natural

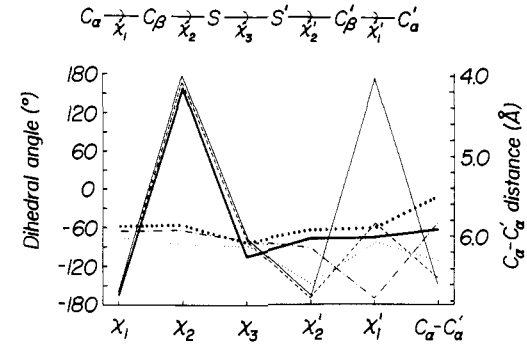

FIGURE 4: Comparison of the geometry of the 9–164 disulfide with those of naturally occurring left-handed disulfides in proteins. All five dihedral angles and C_α–C_α' distances for the disulfides are plotted [after Richardson (1981)]. The geometry of the 9–164 disulfide is shown with a bold line. Cys 9, $\chi_1 = -163$, $\chi_2 = 157$, $\chi_3 = -106$; Cys 164, $\chi_2' = -78$, $\chi_1' = -76$; C_α–$C_\alpha' = 5.9$ Å. The geometries of the five classes of naturally occurring left-handed disulfides are taken from a recent survey (Katz & Kossiakoff, 1986) and are shown in decreasing frequency of occurrence as class 1, thick dotted line; class 2, thin solid line, class 3, dashed line; class 4, chain line; class 5, thin dotted line. The thick dotted line represents the most common conformation of a left-handed spiral.

proteins [cf. Katz and Kossiakoff (1986)]. In the naturally occurring left-handed disulfides, the χ_1 values usually show a trimodal distribution, with the majority in the −60° class, whereas the χ_2 values display a much broader distribution (Richardson, 1981; Thornton, 1981). Thus, the naturally occurring left-handed disulfides adopt one predominant conformation (χ_1, $\chi_1' \simeq -60°$, χ_2, $\chi_2' \simeq -60°$, $\chi_3 \simeq -90°$), and this class of disulfides is thought to be the least strained (Richardson, 1981; Thornton, 1981; Katz & Kossiakoff, 1986). It is apparent from Figure 4 that the dihedral angles (χ_1' and χ_2') of residue 164 adopt the typical left-handed spiral conformation, whereas those of residue 9 (χ_1 and χ_2) do not. Since Cys 164 is located at the C terminus and in the most mobile part of T4 lysozyme, this flexibility might allow it greater freedom to adopt the favorable, and presumably less strained, conformation. In contrast, Cys 9 is within the relatively rigid N-terminal α-helix, and such a side chain might be under configurational constraints that would require the disulfide to adopt a less favorable conformation. This possibility was tested by model-building studies using the program FRODO (Jones, 1978). The study indicated that the conformation of Cys 9 with $\chi_1 = -60°$ would create an unfavorable close approach (2.7 Å) between the sulfur of Cys 164 and the carboxyl oxygen of Glu 5. In addition, it also appeared that the rotation of the side chain would increase the separation between the two sulfurs (S9 and S164) to 2.8 Å, requiring an additional movement of the C-terminal residues of about 1 Å toward Cys 9 to form the disulfide bond (S–S distance of 2.0 Å). Thus, it seems to be difficult for Cys 9 to adopt the ideal χ_1 angle (−60°). It should be emphasized, however, that although the dihedral angles ($\chi_1 = -163°$ and $\chi_2 = 157°$) of Cys 9 are not ideal, these angles have been often observed in naturally occurring disulfides (see Figure 4). Not surprisingly, the engineered protein thus appears to adopt the lowest energy configuration compatible with its local environment, although not the lowest energy dihedral angles expected for a disulfide bridge in isolation.

The present results are in contrast to disulfide bonds engineered into subtilisin (Katz & Kossiakoff, 1986) and dihydrofolate reductase (Villafranca et al., 1987), in which cases rare values of χ_1 and χ_2 were observed.

(2) Strain Energy. Katz and Kossiakoff (1986) have recently analyzed the strain energies in naturally observed di-

sulfide bonds in proteins using an energy expression taken from Weiner et al. (1984). As estimated by this procedure, the naturally occurring left-handed disulfides have strain energies ranging from 0.5 to 4.7 kcal/mol. A similar calculation with the mutant of T4 lysozyme gives a dihedral energy of 4.0 kcal/mol for the 9–164 disulfide bond.

The stability of the 9–164 disulfide bond has been measured by equilibrium studies in a series of redox buffers containing reduced and oxidized DTT (Matsumura et al., 1989a). It was found that the 9–164 disulfide bond is less stable than oxidized DTT by 1.2 kcal/mol. The crystal structure of the oxidized form of DTT has been solved (Capasso & Zagari, 1981), and the observed dihedral angles for this molecule correspond to an estimated strain energy of 2.1 kcal/mol. The calculation therefore indicates that the disulfide of oxidized DTT is more stable than the 9–164 disulfide bond in T4 lysozyme (4.0 kcal/mol). This agrees with the observation that the strain energy (1.2 kcal/mol) of the 9–164 disulfide relative to oxidized DTT in the redox potential experiment is reasonably consistent with the difference between the calculated strain energy of the 9–164 (4.0 kcal/mol) and DTT (2.1 kcal/mol) disulfide bonds. It should be emphasized, however, that the energy calculation is based only on enthalpy, whereas the equilibrium experiment measures the free energy associated with disulfide-bond formation. Also, the calculated strain energies consider only the dihedral angles of the disulfide bond and do not include other factors, such as bond lengths, bond angles, and van der Waals contacts. Nonetheless, our results indicate that simple calculations such as that of Katz and Kossiakoff (1986) can give useful, semiquantitative insights into the amount of strain in a disulfide bond.

(*3*) *Disulfide Solvent Accessibility.* According to the survey by Thornton (1981), most naturally occurring disulfide bonds in proteins are buried, and if such a buried disulfide bond in a protein is reduced, the side-chain volume increases by about 25 Å^3. Such an increase in side-chain volume within the tightly packed interior of a protein would tend to cause unfavorable van der Waals contacts with adjacent residues and be very disruptive. Therefore, it is not surprising that the reduction of buried disulfide bonds tends to be destabilizing (Thornton, 1981; Creighton, 1986). Reduction of such a buried disulfide not only removes the benefit of the chain entropic effect in the denatured state but also disrupts the native state. Conversely, it is possible that naturally occurring buried disulfides stabilize proteins to a greater extent than would be expected solely from the chain entropy effect.

In this context, an exposed disulfide bond is less likely to cause such steric constraints and therefore may be more suitable to evaluate the net effect of the chain entropic effect on protein stabilization. Exposed disulfide bonds can often be reduced without destroying the structure of the protein (Thornton, 1981). Another potential problem is that naturally occurring proteins often contain multiple disulfides, and it may be difficult to differentiate the roles of the individual bridges in such proteins (Creighton, 1986; Pace et al., 1988). In this sense, engineered proteins that contain a single, exposed disulfide bond may have special advantages for biophysical study. In the case of T4 lysozyme the two disulfide bridges that are most effective in increasing the stability of the protein are located on the surface of the molecule and are relatively solvent exposed.

(*B*) *Effect of the Disulfide Bond on Mobility.* How does the introduction of a disulfide bridge alter the dynamics of a protein? Structural studies tend to support the view that the introduction of disulfide bonds need not impose rigidity on a protein structure. Comparison of the wild-type and the 9–164 disulfide lysozymes shows that the overall backbone temperature factors are very similar (Figure 5). A similar result was found in a crystallographic study of a thermostable ribonuclease A that was chemically cross-linked between Lys residues 7 and 41 (Weber et al., 1985). Also, the temperature factor of the β-carbon of Cys 9 in the disulfide mutant (29 Å^2) is higher than the β-carbon of Ile 9 in the wild-type structure (14 Å^2). This loss of rigidity is presumably due to the loss of favorable interactions associated with removal of the Ile 9 side chain, together with possible strain associated with disulfide-bond formation. A similar increase in temperature factors in the vicinity of an engineered disulfide bond was seen for dihydrofolate reductase (Villafranca et al., 1987).

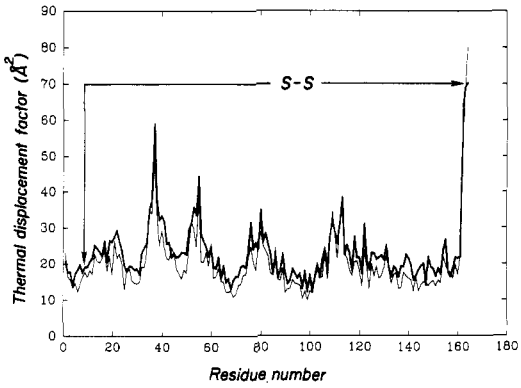

FIGURE 5: Apparent thermal motions of the backbones of WT* and 9C-164C-WT* T4 lysozymes. The value plotted for each residue is the average thermal factor of the backbone atoms N, C$^\alpha$, C, and O. The thick line represents the 9–164 disulfide mutant, and the thin line shows the thermal displacement of pseudo-wild-type lysozyme.

It might have been anticipated that the 9–164 disulfide bond would diminish the motion of the mobile C-terminal segment (residues 162–164) by covalently cross-linking it to the rigid N-terminal α-helix. In contrast, however, the thermal factors of the C-terminal atoms in the disulfide mutant protein were found to be nearly identical with those of wild-type lysozyme (Figure 5). The crystallographic thermal factor B_j for an atom j is related to the mean square amplitude of vibration, $\overline{U_j^2}$, by

$$B_j = 8\pi^2\overline{U_j^2} \quad (1)$$

The derivation of this equation assumes that the atom is vibrating isotopically and that it behaves as a simple harmonic oscillator [e.g., see Lipson and Cochran (1966)]. When B_j becomes large ($\gtrsim$70 Å^2), however, as can occur with atoms in protein crystals, eq 1 is of doubtful value. A thermal factor of B = 70 Å^2 corresponds roughly to a mean displacement of about ±1 Å. In such cases the assumption of isotropic simple harmonic motion becomes very questionable and it is not possible to differentiate between the "thermal motion" and large-scale disorder. Also, once the thermal factor reaches 70 Å^2 or so, it is very poorly determined by the observed X-ray data and is subject to substantial experimental error.

In the present context, the backbone atoms of residues 162–164 in both wild-type and mutant lysozyme have thermal factors in the range 60–80 Å^2 (Figure 5). For the reasons described above, it is not possible to define precisely the nature or the upper limits of this mobility. Therefore, we cannot rule out the possibility that residues 162–164 in wild-type lysozyme are even more disordered than in the mutant structure. What can be said with confidence is that the backbone atoms of residues 162–164 are much more mobile than the rest of the protein backbone even when the 9–164 disulfide bridge is

present. The observation that residues 162–164 retain high mobility in the 9–164 mutant structure is consistent with the belief that disulfide bridges increase the stability of proteins by reducing the backbone configurational entropy of the unfolded state. The nonideal geometry of the disulfide bond, together with loss of rigidity of residue 9, indicates how a loss of favorable interactions as well as the introduction of strain into the folded structure can reduce the net stabilization achieved by a given disulfide bridge.

ACKNOWLEDGMENTS

We thank Drs. L. H. Weaver and D. E. Tronrud for help with data collection and computational aspects. P.E.P. acknowledges the award of an NIH National Research Service Fellowship (GM11836).

REFERENCES

Alber, T., & Matthews, B. W. (1987) *Methods Enzymol. 154*, 511–533.

Anfinsen, C. B., & Scheraga, H. A. (1975) *Adv. Protein Chem. 29*, 205–300.

Capasso, S., & Zagari, A. (1981) *Acta Crystallogr. B37*, 1437–1439.

Chan, H. S., & Dill, K. A. (1989) *J. Chem. Phys. 90*, 492–509.

Creighton, T. E. (1986) *Methods Enzymol. 131*, 83–106.

Flory, P. J. (1956) *J. Am. Chem. Soc. 78*, 5222–5235.

Goldenberg, D. P. (1985) *J. Cell. Biochem. 29*, 321–335.

Goto, Y., & Hamaguchi, K. (1979) *J. Biochem. (Tokyo) 86*, 1433–1441.

Goto, Y., & Hamaguchi, K. (1986) *Biochemistry 25*, 2821–2828.

Goto, Y., Tsunenaga, M., Kawata, Y., & Hamaguchi, K. (1987) *J. Biochem. (Tokyo) 101*, 319–329.

Johnson, R. E., Adams, P., & Rupley, J. A. (1978) *Biochemistry 17*, 1479–1484.

Jones, T. A. (1982) in *Crystallographic Computing* (Sayre, D., Ed.) pp 303–317, Oxford University Press, Oxford, U.K.

Katz, B. A., & Kossiakoff, A. (1986) *J. Biol. Chem. 261*, 15480–15485.

Kunkel, T. A., Roberts, J. D., & Zakour, R. A. (1987) *Methods Enzymol. 154*, 367–382.

Lin, S. H., Konishi, Y., Denton, M. E., & Scheraga, H. A. (1984) *Biochemistry 23*, 5504–5512.

Lin, T.-Y., & Kim, P. S. (1989) *Biochemistry 28*, 5282–5287.

Lipson, H., & Cochran, W. (1966) *The Determination of Crystal Structures, The Crystalline State* (Bragg, L., Ed.) Vol. III, Cornell University Press, Ithaca, NY.

Matsumura, M., & Matthews, B. W. (1989) *Science 243*, 792–794.

Matsumura, M., Becktel, W. J., Levitt, M., & Matthews, B. W. (1989a) *Proc. Natl. Acad. Sci. U.S.A. 86*, 6562–6566.

Matsumura, M., Signor, G., & Matthews, B. W. (1989b) *Nature 342*, 291–293.

Mitchinson, C., & Wells, J. A. (1989) *Biochemistry 28*, 4807–4815.

Muchmore, D. C., McIntosh, L. P., Russell, C. B., Anderson, D. E., & Dahlquist, F. W. (1989) *Methods Enzymol. 177*, 44–73.

Pace, C. N., Grimsley, G. R., Thomson, J. A., & Barnett, B. J. (1988) *J. Biol. Chem. 263*, 11820–11825.

Pantoliano, M. W., Ladner, R. C., Bryan, P. N., Rollence, M. L., Wood, J. F., & Poulos, T. L. (1987) *Biochemistry 26*, 2077–2082.

Perry, L. J., & Wetzel, R. (1984) *Science 226*, 555–557.

Perry, L. J., & Wetzel, R. (1986) *Biochemistry 25*, 733–739.

Poland, D. C., & Scheraga, H. A. (1965) *Biopolymers 3*, 379–399.

Richardson, J. S. (1981) *Adv. Protein Chem. 34*, 167–339.

Rossmann, M. G. (1979) *J. Appl. Crystallogr. 12*, 225–238.

Sauer, R. T., Hehir, K., Stearman, R. S., Weiss, M. A., Jeitler-Nilson, A., Suchanek, E. G., & Pabo, C. O. (1986) *Biochemistry 25*, 5992–5998.

Schellman, J. A. (1955) *C. R. Trav. Lab. Carlsberg, Ser. Chim. 29*, 230–259.

Schmid, M. F., Weaver, L. H., Holmes, M. A., Grütter, M. G., Ohlendorf, D. H., Reynolds, R. A., Remington, S. J., & Matthews, B. W. (1981) *Acta Crystallogr. A37*, 701–710.

Schwarz, H., Hinz, H.-J., Mehlich, A., Tschesche, H., & Wenzel, H. R. (1987) *Biochemistry 26*, 3544–3551.

Thornton, J. M. (1981) *J. Mol. Biol. 151*, 261–287.

Tronrud, D. E., Ten Eyck, L. F., & Matthews, B. W. (1987) *Acta Crystallogr. A43*, 489–501.

Ueda, T., Yamada, H., Hirata, M., & Imoto, T. (1985) *Biochemistry 24*, 6316–6322.

Villafranca, J. E., Howell, E. E., Voet, D. H., Strobel, M. S., Ogden, R. C., Abelson, J. N., & Kraut, J. (1983) *Science 222*, 782–788.

Villafranca, J. E., Howell, E. E., Oatley, S. J., Xuong, N., & Kraut, J. (1987) *Biochemistry 26*, 2182–2189.

Weaver, L. H., & Matthews, B. W. (1987) *J. Mol. Biol. 193*, 189–199.

Weber, P. C., Sheriff, S., Ohlendorf, D. H., Finzel, B. C., & Salemme, F. R. (1985) *Proc. Natl. Acad. Sci. U.S.A. 82*, 8473–8477.

Weiner, S. J., Kollman, P. A., Case, D. A., Singh, U. C., Ghio, C., Alagona, G., Profeta, S., & Weiner, P. (1984) *J. Am. Chem. Soc. 106*, 765–784.

Wells, J. A., & Powers, D. B. (1986) *J. Biol. Chem. 261*, 6564–6570.

Wetzel, R., Perry, L. J., Baase, W. A., & Becktel, W. J. (1988) *Proc. Natl. Acad. Sci. U.S.A. 85*, 401–405.